CLASSIFICATION: Biological Sciences, Neuroscience

Tryptophan-2,3-dioxygenase (TDO) inhibition ameliorates neurodegeneration by modulation of kynurenine pathway metabolites

Carlo Breda[1], Korrapati V. Sathyasaikumar[2], Shama Sograte Idrissi[1], Francesca M. Notarangelo[2], Jasper G. Estranero[1], Gareth G. L. Moore[1], Edward W Green[1], Charalambos P. Kyriacou[1], Robert Schwarcz[2] and Flaviano Giorgini[1]

[1]Department of Genetics, University of Leicester, University Road, Leicester LE1 7RH, UK

[2]Maryland Psychiatric Research Center, Department of Psychiatry, University of Maryland School of Medicine, Baltimore, MD 21228, USA

Corresponding Author:
Flaviano Giorgini,
Department of Genetics, University of Leicester, Leicester, LE1 7RH, UK
Email: fg36@le.ac.uk
Telephone: +441162523378

SHORT TITLE: TDO inhibition ameliorates neurodegeneration

KEYWORDS: neurodegeneration, KMO, TDO, Parkinson's disease, Alzheimer's disease

ABSTRACT

Metabolites of the kynurenine pathway (KP) of tryptophan (TRP) degradation have been closely linked to the pathogenesis of several neurodegenerative disorders. Recent work has highlighted the therapeutic potential of inhibiting two critical regulatory enzymes in this pathway - kynurenine 3-monooxygenase (KMO) and tryptophan-2,3-dioxygenase (TDO). Much evidence indicates that the efficacy of KMO inhibition arises from normalizing an imbalance between neurotoxic [3-hydroxykynurenine (3-HK); quinolinic acid (QUIN)] and neuroprotective [kynurenic acid (KYNA)] KP metabolites. However, it is not clear if TDO inhibition is protective via a similar mechanism or if this is instead due to increased levels of TRP - the substrate of TDO. Here, we find that increased levels of KYNA relative to 3-HK are likely central to the protection conferred by TDO inhibition in a fruit fly model of Huntington's disease and that TRP treatment strongly reduces neurodegeneration by shifting KP flux towards KYNA synthesis. In fly models of Alzheimer's and Parkinson's disease, we provide the first genetic evidence that inhibition of TDO or KMO reduces neurodegeneration, improves locomotor performance and ameliorates shortened lifespan. Critically, we find that treatment with a chemical TDO inhibitor is robustly protective in these models. Consequently, our work strongly supports targeting of the KP as a potential treatment strategy for several major neurodegenerative disorders, and suggests that alterations in the levels of neuroactive KP metabolites could underlie any therapeutic benefits.

SIGNIFICANCE STATEMENT

Neurodegenerative disorders such as Alzheimer's (AD), Parkinson's (PD), and Huntington's (HD) diseases present a significant and increasing burden on society. Perturbations in the kynurenine pathway (KP) of tryptophan degradation have been linked to the pathogenesis of these disorders, and thus manipulation of this pathway may have therapeutic relevance. Here we show that genetic inhibition of two kynurenine pathway (KP) enzymes – KMO and TDO – improved neurodegeneration and other disease symptoms in fruit fly models of AD, PD, and HD, and that alterations in levels of neuroactive KP metabolites likely underlie the beneficial effects. Furthermore, we find that inhibition of TDO using a drug-like compound reverses several disease phenotypes, underscoring the therapeutic promise of targeting this pathway in neurodegenerative disease.

\body

INTRODUCTION

The kynurenine pathway (KP), the major catabolic route of tryptophan (TRP) metabolism in mammals (Figure 1), has been closely linked to the pathogenesis of several brain disorders (1). This pathway contains several neuroactive metabolites, including 3-hydroxykynurenine (3-HK), quinolinic acid (QUIN) and kynurenic acid (KYNA) (2). QUIN is a well-characterized endogenous neurotoxin that specifically activates N-methyl-D-aspartate (NMDA) receptors, thereby inducing excitotoxicity (3, 4). 3-HK and QUIN are also neurotoxic via the generation of free radicals and oxidative stress (5, 6). Conversely, KYNA – synthesized by kynurenine aminotransferases (KATs) - is neuroprotective through its antioxidant properties and antagonism of both the α7 nicotinic acetylcholine receptor and the glycine co-agonist site of the NMDA receptor (7-13). Levels of these metabolites are regulated at two critical points in the KP: 1) the initial, rate-limiting conversion of TRP into N-formylkynurenine by either tryptophan-2,3-dioxygenase (TDO) or indoleamine-2,3-dioxygenase 1 and 2 (IDO1, IDO2); and 2) synthesis of 3-HK from kynurenine by the flavoprotein kynurenine 3-monoxygenase (KMO) (1).

Alterations in the levels of the KP metabolites have been observed in a broad range of brain disorders, including both neurodegenerative and psychiatric conditions (14). In neurodegenerative diseases such as Huntington's (HD), Parkinson's (PD) and Alzheimer's (AD), a shift towards increased synthesis of the neurotoxic metabolites QUIN and 3-HK relative to KYNA may contribute to disease (1). Indeed, in HD patients and HD model mice 3-HK and QUIN levels are increased in the neostriatum and cortex (15, 16). Moreover, KYNA levels are reduced in the striatum of HD patients (17). Several studies have also found perturbation in KP metabolites in the blood and cerebrospinal fluid of AD patients, with decreased levels of KYNA correlating with reduced cognitive performance (18, 19). Similarly, in the basal ganglia of PD patients a reduction in KYNA levels combined with increased 3-HK has been observed (20, 21).

Drosophila melanogaster has provided a useful model for interrogation of the KP in both normal physiology and in neurodegenerative disease (22, 23). In fruit flies, TDO and

KMO are encoded by *vermillion* (*v*) and *cinnabar* (*cn*), respectively, and both are implicated in *Drosophila* eye colour pigmentation and brain plasticity (24, 25). In flies, TDO is the sole enzyme that catalyzes the initial step of the KP, as IDO1 and IDO2 are not present (see Figure 1), and so provides a distinctive model for examining the role of this critical step in the pathway. Moreover, we have previously found that down-regulating *cn* and *v* gene expression significantly reduces neurodegeneration in flies expressing a mutant huntingtin (HTT) fragment – the central causative insult underlying HD (22). We also observed that pharmacological manipulations that reduced the 3-HK/KYNA ratio were always associated with neuroprotection. Notably, re-introduction of physiological levels of 3-HK in HD flies which lacked this metabolite due to KMO inhibition was sufficient to abolish neuroprotection (22). Furthermore, in a *C. elegans* model of PD, genetic down-regulation of TDO ameliorates α-synuclein (aSyn) toxicity (26). This effect appeared to be independent of changes in the levels of serotonin or KP metabolites but was correlated with increased TRP levels. Supplementing worms with TRP also suppressed aSyn-dependent phenotypes (26). The present study was designed to further define the mechanism(s) that underlie the neuroprotection conferred by TRP treatment and TDO inhibition, and to extend our analyses of the neuroprotective potential of the KP to fruit fly models of AD and PD.

RESULTS

TRP is neuroprotective in HD flies via modulation of downstream KP metabolites

As work in *C. elegans* suggests that TDO inhibition and TRP treatment may confer protection against toxicity arising from misfold proteins *independent* of KP metabolites (26), here we investigated whether alterations in KP metabolites was central to this protection in HD flies. These flies feature the pan-neuronal expression of a mutant HTT exon 1 encoding fragment (HTT93Q) under control of the *elav*GAL4 pan-neuronal driver, and serve as a well-characterized model of HD (27). In particular, degeneration of photoreceptor neurons (rhabdomeres) in the eye serves as a robust and reproducible readout for neurodegeneration, which can be easily scored using the pseudopupil assay. HTT93Q flies were allowed to develop on media supplemented with various concentrations of TRP (from 0.4 to 10 mg/ml), and neurodegeneration was assessed at day 0 on newly emerged flies. TRP supplementation resulted in a dose-dependent amelioration of neurodegeneration compared to untreated controls, with 0.8 mg/ml being the minimum protective concentration ($P < 0.001$), and the protection saturating at 3.5 mg/ml TRP ($P < 0.001$; Figure 2A). In order to assess whether TRP-induced neuroprotection was dependent upon changes in downstream neuroactive KP metabolites, we next determined the levels of the neurotoxic metabolite 3-HK and the neuroprotective metabolite KYNA. TRP treatment of HTT93Q flies substantially reduced levels of 3-HK relative to KYNA ($P < 0.001$; Figure 2B), predominantly driven by increased levels of KYNA (Figure S1A and S1B). Furthermore, we observed that the low level of emergence of adult HD flies from the pupal case (eclosion; Figure S1C) was significantly enhanced by feeding of 3.5 mg/ml TRP ($P < 0.001$; Figure 2C). These data suggest that the neuroprotection conferred by TRP treatment is due – at least in part – to increased levels of KYNA in these flies.

We next explored the mechanism(s) by which TDO inhibition leads to neuroprotection. First, HTT93Q flies carrying a strong amorphic allele of *v* (v^{36f}) were employed to assess the role of KYNA. These $v^{-/-}$ HTT93Q flies exhibit a dramatic ~8-fold increase in TRP levels compared to controls ($P < 0.001$; Figure 2D), as well as a significant ~80% reduction in the 3-HK/KYNA ratio ($P < 0.001$; Figure 2E, S1D, E). To reduce levels of KYNA in the HTT93Q $v^{-/-}$ background, we used the non-specific KAT inhibitor aminooxyacetic

acid (AOAA), which effectively reduces KYNA synthesis in rodents *in vitro* and *in vivo* (28, 29). Animals administered 100 µM of AOAA in their food exhibited a significant decrease in KYNA levels ($P < 0.05$; Figure 2F), which resulted in an increase in the 3-HK/KYNA ratio ($P < 0.05$; Figure 2G). Strikingly, these animals showed a complete reversal of the neuroprotection conferred by TDO inhibition ($P < 0.001$; Figure 2H). No changes were seen in levels of TRP or 3-HK (Figure S1F, G), so these findings strongly suggest that KYNA is central to the neuroprotection observed.

We next asked whether modulation in 3-HK levels, too, plays a role in the neuroprotection observed in TDO-deficient flies, which have greatly reduced 3-HK levels (22)(Figure 2I). In line with our demonstration that re-introduction of 3-HK in KMO-deficient flies ($cn^{-/-}$) is sufficient to restore neurodegeneration (22), we administered several concentrations of 3-HK (0.2 to 1 mg/ml) to the flies in the food (Figure 2I, J). Surprisingly, we found that - unlike $cn^{-/-}$ HTT93Q flies (22) - restoration of physiological levels of 3-HK in $v^{-/-}$ HTT93Q flies (at the 0.2 mg/ml dose) did not reverse neuroprotection (Figure 2J). Increasing 3-HK to hyperphysiological levels via administration of 1 mg/ml 3-HK enhanced neurodegeneration in $v^{-/-}$ HTT93Q flies, thereby eliminating the neuroprotection normally observed ($P < 0.001$; Figure 2J). In all cases, we found that 3-HK treatment led to significant increases in the 3-HK/KYNA ratio (Figure S1H, I). Thus, restoration of physiological 3-HK levels is *not* sufficient to abrogate the neuroprotection conferred in TDO-deficient flies.

The excitotoxin QUIN promotes neurodegeneration in *Drosophila*

Drosophila does not express the KP enzyme 3-hydroxyanthranilic acid dioxygenase, and thus fruit flies do not synthesize QUIN (30). Therefore we fed *elavGAL4*-driven HTT93Q flies with increasing QUIN concentrations during development and assessed neurodegeneration by scoring the number of rhabdomeres at day 0. We first measured QUIN in wild-type (WT) and HD fly heads. As expected, QUIN was detected in flies fed with 0.5 mg/ml QUIN, but not in the untreated group ($P < 0.001$; Figure 3A). Interestingly, we found that HTT93Q flies accumulate more QUIN than WT flies ($P < 0.01$). While QUIN feeding did not cause degeneration of rhabdomeres in WT flies (Figure S2A), QUIN treatment (0.2 and 0.5 mg/ml) enhanced neurodegeneration in HTT93Q flies in a dose-dependent manner (Figure 3B).

Notably, KMO inhibition did not protect against QUIN-induced neurotoxicity in HTT93Q flies carrying homozygous cn^3 mutation, a strong amophic *cn* allele (Figure 3B).

Endogenous synthesis of KYNA in fruit flies is neuroprotective

We next generated a *Drosophila* line carrying a transgene encoding hKAT – (*UAS-hKAT*), the KP enzyme which converts kynurenine to KYNA (Figure 1). In wild-type flies, pan-neuronal hKAT expression driven by *elav*GAL4 caused a dramatic increase in KYNA levels at both day 1 and day 7 when compared to controls ($P < 0.001$; Figure 3C), and in HD flies dramatically reduced the 3-HK/KYNA ratio at day 1 and day 7 post-eclosion ($P < 0.01$; Figure 3D, S2B, C). This effect was associated with a significant amelioration of both rhabdomere neurodegeneration ($P < 0.001$; Figure 3E) and impaired eclosion in HTT93Q flies ($P < 0.001$; Figure 3F).

KMO and TDO inhibition ameliorates disease phenotypes in fly models of PD and AD

As both KMO and TDO inhibition were robustly protective in HD model fruit flies, we tested the efficacy of these approaches in *Drosophila* models of PD and AD. For recapitulating these disorders, we employed transgenic fly lines expressing human aSyn as a model of PD (31) and the human $A\beta_{42}$ peptide [either WT or the Arctic mutant form (E693G), which causes autosomal dominant AD - $A\beta_{42Arc}$] as a model of AD (32, 33). We employed RNA interference (RNAi) to down-regulate expression of the genes encoding either TDO (*v*) or KMO (*cn*), and found a dramatic reduction in the 3-HK/KYNA ratio, mainly due to increased synthesis of KYNA ($P < 0.001$; Figure 4H and Figure S3B,C). TRP levels were not significantly altered by these manipulations (Figure S3A), which reduce *cn* and *v* expression by ~80-95% (22).

For both models, we first assessed larval crawling as an indication of behavioral impairments during early developmental stages (34). Expression of either aSyn or $A\beta_{42Arc}$ in motor neurons using the *c164GAL4* driver led to a reduction in the distance crawled by third instar larvae ($P < 0.001$; Figure 4A and B, respectively). The down-regulation of the genes encoding either TDO (*v*) or KMO (*cn*) by RNA interference significantly enhanced crawling behavior in both models (aSyn: $P < 0.01$; $A\beta_{42Arc}$ $P < 0.001$).

As the expression of aSyn shortens lifespan compared to control flies (35), we next assessed lifespan upon pan-neuronal expression of either aSyn or $A\beta_{42}$ constructs. We observed a small but significant improvement in the shortening of median lifespan in aSyn flies in which either TDO (*v*) or KMO (*cn*) had been silenced ($P < 0.001$, Figure 4C). Notably, silencing of either of the two enzymes also significantly ameliorated shortened median lifespan in $A\beta_{42}$ flies from 54 to 66 and 68 days, respectively ($P < 0.001$, Figure 4D). Complementing this observation, *cn* down-regulation also significantly reversed shortened lifespan in the $A\beta_{42Arc}$ model ($P < 0.001$, Figure S4A).

Locomotor behavior in adult flies was assessed by examining negative geotaxis ability (climbing) as a measurement of motor impairment. *elav*GAL4-driven aSyn, $A\beta_{42}$ and $A\beta_{42Arc}$ flies exhibited a reduction in climbing at all the post-eclosion ages tested (Figures 4E,F and S4B). Silencing of either TDO or KMO improved climbing ability in all these models (Figures 4E,F and S4B). Notably, scoring the number of rhabdomeres per ommatidium revealed that genetic knockdown of either enzyme also consistently reduced neurodegeneration in *elav*GAL4-driven $A\beta_{42Arc}$ flies at all ages tested ($P < 0.01$, Figure 4G).

Finally, we interrogated the effect of pharmacological TDO inhibition in the three fly models of neurodegeneration, using the commercially available TDO inhibitor 680C91 (36). Feeding of 680C91 (100 µM) to newly emerged HTT93Q flies resulted in dramatically reduced neurodegeneration 7 days post-eclosion compared with flies fed vehicle alone (Figure 5A, $P < 0.001$). In PD and AD flies, pharmacological inhibition of TDO with 100 µM 680C91 led to a significant amelioration in climbing performance when compared to respective controls 10 days post-eclosion (Figure 5B, $P < 0.001$).

DISCUSSION

Impairments in KP metabolism have been linked to several neurodegenerative disorders, and in particular to the pathogenesis of HD (37). Notably, increased levels of 3-HK and QUIN have been measured in the neostriatum and cortex of early stage HD patients (15), and these changes are associated with an up-regulation of *IDO1* transcription (38) and a reduction in the activity of KAT, which is critical for KYNA synthesis (17). These data in HD patients are supported by observations in HD mice, which show increased cerebral KMO activity (39). We previously found that either genetic or pharmacological inhibition of KMO is protective in HD flies and leads to a corresponding increase in KYNA levels relative to 3-HK (22). Furthermore, we reported that KYNA treatment reduced neurodegeneration in these flies. Here, we have extended this work by generating transgenic flies which overexpress hKAT and thereby synthesize ~20-fold more KYNA than control flies. This increased formation of KYNA reduced neurodegeneration and eclosion defects in HD model flies. Furthermore, KMO inhibition by RNAi revealed beneficial effects in several behavioral and disease-relevant outcome measures, including larval crawling, longevity, climbing, and rhabdomere degeneration, in AD and PD model flies. These results strongly support the notion that KMO inhibition has relevance as a treatment strategy in a broad range of neurodegenerative diseases. In addition, these data also suggest that the design of small molecules capable of increasing KAT activity could have therapeutic relevance for neurodegenerative disorders.

The present results, demonstrating that both genetic and pharmacological inhibition of TDO provides robust neuroprotection in fly models of AD and PD, also confirmed and extended the results of our previous study, which had identified TDO as a candidate drug target in HD flies (22). These protective effects are associated with a decrease in the 3-HK/KYNA ratio, i.e. a shift towards increased KYNA synthesis. Work in *C. elegans* has revealed that TDO inhibition is also protective in models of proteotoxicity, although amelioration of the phenotypes occurred independently of changes in the levels of KP metabolites and was instead associated with elevated TRP levels (26). Although the underlying mechanism remained unclear, the favorable effects of high TRP levels in the nematode were substantiated by the fact that TRP treatment conferred robust protection from disease-related phenotypes (Figure 1). In the present study, too, TRP supplementation

of the diet was effective, ameliorating rhabdomere degeneration and eclosion defects in HD flies. However, TRP feeding was also associated with a reduction in the 3-HK/KYNA ratio, suggesting that the protective effects of the amino acid may be linked to an increase in the production of the neuroprotective metabolite KYNA (Figure 1). Indeed, partial inhibition of KYNA synthesis in TDO-deficient flies proved sufficient to completely reverse neuroprotection. In addition, restoration of physiological 3-HK levels in TDO-deficient HD flies did not reverse neuroprotection, in contrast to KMO-deficient flies (22). In primary neurons, 3-HK toxicity is dependent upon its uptake via neutral amino acid transporters, and co-application of TRP can block this toxicity by competing for the same transporters (6). Thus, it is possible that the vast excess of TRP observed in the heads of HTT93Q $v^{-/-}$ flies (~8-fold versus controls) competes with 3-HK for rhabdomere uptake, thereby requiring hyperphysiological levels of 3-HK to reverse TDO-dependent neuroprotection. A similar mechanism may also contribute to the neuroprotection observed with TRP treatment in general. Herein, we have also found that RNAi knockdown of either *cn* or *v* does not increase TRP levels, and thus the neuroprotection observed in the AD and PD flies strongly correlates with a decrease in the 3-HK/KYNA ratio. The mechanism causing TRP treatment to favor KYNA synthesis over the formation of 3-HK in *Drosophila*, as well as the unexpected qualitative differences in the effects of TDO inhibition and TRP administration on KP metabolism between fruit flies and nematodes, clearly requires further investigation.

Interestingly, we found that QUIN – which is not normally synthesized in fruit flies (40) – potentiated neurodegeneration in HD flies, and reversed the protective effects of KMO inhibition. As the same QUIN treatment did not cause neuron loss in wild-type flies, mutant HTT may potentiate vulnerability by enhancing NMDA receptor function (41, 42) and/or by increasing susceptibility to toxic free radicals (43), i.e. by augmenting the two major mechanisms known to be involved in QUIN-induced neurotoxicity (44). If verified in mammals, a reduction in brain QUIN levels - along with a decrease in 3-HK levels – relative to KYNA could therefore be especially promising in the treatment of HD (45). Our observation of increased levels of QUIN in HTT93Q versus WT flies is enigmatic, but may be due to altered feeding behavior, increased permeability of the blood-brain barrier (46, 47), or differences in KP metabolism, and would be interesting to explore in future studies.

In conclusion, the present set of experiments further validates the hypothesis that

KP metabolism is causally linked to neuronal viability and that modulation of the KP constitutes a promising therapeutic strategy for a variety of major neurodegenerative disorders. Notably, we provide the first genetic evidence that KMO inhibition is protective in animal models of PD and AD and that pharmacological targeting of TDO is also neuroprotective. We have clarified the mechanism underlying the protective effects of TDO inhibition, which will stimulate efforts to target this step of the KP in neurodegenerative disease. These results, together with supportive studies in flies (48) and rodents (49), raise the possibility that inhibition of TDO and KMO – or combinatorial treatment - may offer therapeutic advantages. The availability of new TDO inhibitors (50, 51), and access to the crystal structures of both TDO (52) and KMO (53), should allow further testing of these hypotheses in the near future.

MATERIALS AND METHODS

Drosophila strains

Fruit flies were maintained on standard maize food at 25°C in a light/dark cycle of 12:12 hours. The *elavGAL4* [c155], *w*; +; *UASaSyn* (8146), *w*; +; *UASA*β_{42} (32037), *w*; +; *UASA*β_{42Arc} (33774), cn^3 and v^{36f} null fly stocks were obtained from the Bloomington Drosophila Stock Center (Bloomington, Indiana). The *c164GAL4* driver line was a gift from Juan Botas (Baylor College of Medicine). HTT93Q exon 1 flies (27) were a gift from Larry Marsh and Leslie Thompson (University of California, Irvine). *cn* and *v* RNAi lines are part of the phiC31 RNAi Library (KK) and were obtained from the Vienna *Drosophila* RNAi Center (54).

The gene encoding kynurenine aminotransferase (hKAT) was amplified from a human fetal cDNA library (55) and cloned into the pJFRC2 vector (56) – a gift from Gerald Rubin (Addgene plasmid #26214) - by standard methods. The resulting construct was injected by BestGene Inc. into attP40 *Drosophila* strains (57).

Pseudopupil analysis, eclosion analysis, feeding experiments, measurement of KP metabolites, behavioral assays, longevity analysis, and statistical analyses are described in detail in SI Materials and Methods. Measurement of KP metabolites in treated flies was performed at either 0 or 7 days post-eclosion.

Acknowledgements

We thank BestGene Inc. for the generation of transgenic lines. We gratefully acknowledge the gift of transgenic fly lines from J. Lawrence Marsh, Leslie Thompson and Juan Botas. CB was supported by grants from the CHDI Foundation and Parkinson's UK to FG and CPK. FG and CPK also acknowledge grants from the Medical Research Council (MRC) and the Biotechnology and Biological Sciences Research Council (BBSRC) for valuable infrastructure supporting this work. Work in the Schwarcz laboratory was supported by NIH grant RO1-NS057715.

REFERENCES

1. Amaral M, Outeiro TF, Scrutton NS, & Giorgini F (2013) The causative role and therapeutic potential of the kynurenine pathway in neurodegenerative disease. *J Mol Med (Berl)* 91(6):705-713.
2. Thevandavakkam MA, Schwarcz R, Muchowski PJ, & Giorgini F (2010) Targeting kynurenine 3-monooxygenase (KMO): implications for therapy in Huntington's disease. *CNS Neurol Disord Drug Targets* 9(6):791-800.
3. Stone TW & Perkins MN (1981) Quinolinic acid: a potent endogenous excitant at amino acid receptors in CNS. *Eur J Pharmacol* 72(4):411-412.
4. Schwarcz R, Whetsell WO, Jr., & Mangano RM (1983) Quinolinic acid: an endogenous metabolite that produces axon-sparing lesions in rat brain. *Science* 219(4582):316-318.
5. Okuda S, Nishiyama N, Saito H, & Katsuki H (1996) Hydrogen peroxide-mediated neuronal cell death induced by an endogenous neurotoxin, 3-hydroxykynurenine. *Proc Natl Acad Sci U S A* 93(22):12553-12558.
6. Okuda S, Nishiyama N, Saito H, & Katsuki H (1998) 3-Hydroxykynurenine, an endogenous oxidative stress generator, causes neuronal cell death with apoptotic features and region selectivity. *J Neurochem* 70(1):299-307.
7. Goda K, Hamane Y, Kishimoto R, & Ogishi Y (1999) Radical scavenging properties of tryptophan metabolites. Estimation of their radical reactivity. *Adv Exp Med Biol* 467:397-402.
8. Foster AC, Vezzani A, French ED, & Schwarcz R (1984) Kynurenic acid blocks neurotoxicity and seizures induced in rats by the related brain metabolite quinolinic acid. *Neurosci Lett* 48(3):273-278.
9. Carpenedo R*, et al.* (2001) Presynaptic kynurenate-sensitive receptors inhibit glutamate release. *Eur J Neurosci* 13(11):2141-2147.
10. Hilmas C*, et al.* (2001) The brain metabolite kynurenic acid inhibits alpha7 nicotinic receptor activity and increases non-alpha7 nicotinic receptor expression: physiopathological implications. *J Neurosci* 21(19):7463-7473.
11. Perkins MN & Stone TW (1982) An iontophoretic investigation of the actions of convulsant kynurenines and their interaction with the endogenous excitant quinolinic acid. *Brain Res* 247(1):184-187.
12. Hardeland R*, et al.* (1999) Indole-3-pyruvic and -propionic acids, kynurenic acid, and related metabolites as luminophores and free-radical scavengers. *Adv Exp Med Biol* 467:389-395.
13. Lugo-Huitron R*, et al.* (2011) On the antioxidant properties of kynurenic acid: free radical scavenging activity and inhibition of oxidative stress. *Neurotoxicol Teratol* 33(5):538-547.
14. Schwarcz R, Bruno JP, Muchowski PJ, & Wu HQ (2012) Kynurenines in the mammalian brain: when physiology meets pathology. *Nat Rev Neurosci* 13(7):465-477.
15. Guidetti P, Luthi-Carter RE, Augood SJ, & Schwarcz R (2004) Neostriatal and cortical quinolinate levels are increased in early grade Huntington's disease. *Neurobiol Dis* 17(3):455-461.
16. Guidetti P*, et al.* (2006) Elevated brain 3-hydroxykynurenine and quinolinate levels in Huntington disease mice. *Neurobiol Dis* 23(1):190-197.
17. Jauch D*, et al.* (1995) Dysfunction of brain kynurenic acid metabolism in Huntington's disease: focus on kynurenine aminotransferases. *J Neurol Sci* 130(1):39-47.
18. Hartai Z*, et al.* (2007) Decreased serum and red blood cell kynurenic acid levels in Alzheimer's disease. *Neurochem Int* 50(2):308-313.
19. Heyes MP*, et al.* (1992) Quinolinic acid and kynurenine pathway metabolism in inflammatory and non-inflammatory neurological disease. *Brain* 115 (Pt 5):1249-1273.
20. Knyihar-Csillik E*, et al.* (2006) Effect of 6-hydroxydopamine treatment on kynurenine aminotransferase-I (KAT-I) immunoreactivity of neurons and glial cells in the rat substantia nigra. *Acta Neuropathol* 112(2):127-137.

21. Ogawa T*, et al.* (1992) Kynurenine pathway abnormalities in Parkinson's disease. *Neurology* 42(9):1702-1706.
22. Campesan S*, et al.* (2011) The kynurenine pathway modulates neurodegeneration in a Drosophila model of Huntington's disease. *Curr Biol* 21(11):961-966.
23. Green EW*, et al.* (2012) Drosophila eye color mutants as therapeutic tools for Huntington disease. *Fly (Austin)* 6(2):117-120.
24. Tearle R (1991) Tissue specific effects of ommochrome pathway mutations in Drosophila melanogaster. *Genet Res* 57(3):257-266.
25. Savvateeva E*, et al.* (2000) Age-dependent memory loss, synaptic pathology and altered brain plasticity in the Drosophila mutant cardinal accumulating 3-hydroxykynurenine. *J Neural Transm* 107(5):581-601.
26. van der Goot AT*, et al.* (2012) Delaying aging and the aging-associated decline in protein homeostasis by inhibition of tryptophan degradation. *Proc Natl Acad Sci U S A* 109(37):14912-14917.
27. Steffan JS*, et al.* (2001) Histone deacetylase inhibitors arrest polyglutamine-dependent neurodegeneration in Drosophila. *Nature* 413(6857):739-743.
28. Turski WA, Gramsbergen JB, Traitler H, & Schwarcz R (1989) Rat brain slices produce and liberate kynurenic acid upon exposure to L-kynurenine. *J Neurochem* 52(5):1629-1636.
29. Speciale C*, et al.* (1990) Determination of extracellular kynurenic acid in the striatum of unanesthetized rats: effect of aminooxyacetic acid. *Neurosci Lett* 116(1-2):198-203.
30. Linzen B (1974) Tryptophan - Ommochrome Pathway in Insects. *Advances in Insect Physiology* 10:117–246.
31. Feany MB & Bender WW (2000) A Drosophila model of Parkinson's disease. *Nature* 404(6776):394-398.
32. Murakami K*, et al.* (2002) Synthesis, aggregation, neurotoxicity, and secondary structure of various A beta 1-42 mutants of familial Alzheimer's disease at positions 21-23. *Biochem Biophys Res Commun* 294(1):5-10.
33. Nilsberth C*, et al.* (2001) The 'Arctic' APP mutation (E693G) causes Alzheimer's disease by enhanced Abeta protofibril formation. *Nat Neurosci* 4(9):887-893.
34. Nishimura Y*, et al.* (2010) Selection of Behaviors and Segmental Coordination During Larval Locomotion Is Disrupted by Nuclear Polyglutamine Inclusions in a New Drosophila Huntington's Disease-Like Model. *Journal of Neurogenetics* 24(4):194-206.
35. Breda C*, et al.* (2015) Rab11 modulates alpha-synuclein-mediated defects in synaptic transmission and behaviour. *Hum Mol Genet* 24(4):1077-1091.
36. Salter M, Hazelwood R, Pogson CI, Iyer R, & Madge DJ (1995) The effects of a novel and selective inhibitor of tryptophan 2,3-dioxygenase on tryptophan and serotonin metabolism in the rat. *Biochem Pharmacol* 49(10):1435-1442.
37. Maddison DC & Giorgini F (2015) The kynurenine pathway and neurodegenerative disease. *Semin Cell Dev Biol*.
38. Mazarei G*, et al.* (2010) Expression analysis of novel striatal-enriched genes in Huntington disease. *Hum Mol Genet* 19(4):609-622.
39. Sathyasaikumar KV*, et al.* (2010) Dysfunctional kynurenine pathway metabolism in the R6/2 mouse model of Huntington's disease. *J Neurochem* 113(6):1416-1425.
40. Linzen B (1974) Tryptophan-ommochrome pathway in insects. *Advances in Insect Physiology* 10:117–246.
41. Ultsch A, Schuster CM, Laube B, Betz H, & Schmitt B (1993) Glutamate receptors of Drosophila melanogaster. Primary structure of a putative NMDA receptor protein expressed in the head of the adult fly. *FEBS Lett* 324(2):171-177.
42. Zachepilo TG*, et al.* (2008) Comparative analysis of the locations of the NR1 and NR2 NMDA receptor subunits in honeybee (Apis mellifera) and fruit fly (Drosophila melanogaster, Canton-S wild-type) cerebral ganglia. *Neurosci Behav Physiol* 38(4):369-372.

43. Wang CT*, et al.* (2012) Reduced neuronal expression of ribose-5-phosphate isomerase enhances tolerance to oxidative stress, extends lifespan, and attenuates polyglutamine toxicity in Drosophila. *Aging Cell* 11(1):93-103.
44. Pérez-De La Cruz V & Santamaria A (2007) Integrative hypothesis for Huntington's disease: a brief review of experimental evidence. *Physiol Res* 56(5):513-526.
45. Guidetti P & Schwarcz R (1999) 3-Hydroxykynurenine potentiates quinolinate but not NMDA toxicity in the rat striatum. *Eur J Neurosci* 11(11):3857-3863.
46. Drouin-Ouellet J*, et al.* (2015) Cerebrovascular and blood-brain barrier impairments in Huntington's disease: Potential implications for its pathophysiology. *Ann Neurol* 78(2):160-177.
47. Schirmeier S & Klämbt C (2015) The Drosophila blood-brain barrier as interface between neurons and hemolymph. *Mech Dev* 138 Pt 1:50-55.
48. Oxenkrug GF, Navrotskaya V, Voroboyva L, & Summergrad P (2011) Extension of life span of Drosophila melanogaster by the inhibitors of tryptophan-kynurenine metabolism. *Fly (Austin)* 5(4):307-309.
49. Zwilling D*, et al.* (2011) Kynurenine 3-monooxygenase inhibition in blood ameliorates neurodegeneration. *Cell* 145(6):863-874.
50. Reniers J*, et al.* (2011) Synthesis and inhibition study of monoamine oxidase, indoleamine 2,3-dioxygenase and tryptophan 2,3-dioxygenase by 3,8-substituted 5H-indeno[1,2-c]pyridazin-5-one derivatives. *Eur J Med Chem* 46(12):6104-6111.
51. Dolusic E*, et al.* (2011) Tryptophan 2,3-dioxygenase (TDO) inhibitors. 3-(2-(pyridyl)ethenyl)indoles as potential anticancer immunomodulators. *J Med Chem* 54(15):5320-5334.
52. Huang W, Gong Z, Li J, & Ding J (2013) Crystal structure of Drosophila melanogaster tryptophan 2,3-dioxygenase reveals insights into substrate recognition and catalytic mechanism. *J Struct Biol* 181(3):291-299.
53. Amaral M*, et al.* (2013) Structural basis of kynurenine 3-monooxygenase inhibition. *Nature* 496(7445):382-385.
54. Green EW, Fedele G, Giorgini F, & Kyriacou CP (2014) A Drosophila RNAi collection is subject to dominant phenotypic effects. *Nat Methods* 11(3):222-223.
55. Thaminy S, Auerbach D, Arnoldo A, & Stagljar I (2003) Identification of novel ErbB3-interacting factors using the split-ubiquitin membrane yeast two-hybrid system. *Genome Res* 13(7):1744-1753.
56. Pfeiffer BD*, et al.* (2010) Refinement of tools for targeted gene expression in Drosophila. *Genetics* 186(2):735-755.
57. Markstein M, Pitsouli C, Villalta C, Celniker SE, & Perrimon N (2008) Exploiting position effects and the gypsy retrovirus insulator to engineer precisely expressed transgenes. *Nat Genet* 40(4):476-483.

FIGURE LEGENDS

Figure 1. Consequences of kynurenine pathway (KP) manipulation. KP metabolites and enzymatic steps are indicated in black, while the key KP enzymes tryptophan-2,3-dioxygenase (TDO), kynurenine 3-monooxygenase (KMO) and kynurenine aminotransferases (KATs) are indicated in purple. The metabolites 3-hydroxykynurenine (3-HK) and quinolinic acid (QUIN) are neurotoxic (as indicated by red arrows), while kynurenic acid (KYNA) and tryptophan (TRP) are neuroprotective (as indicated by green arrows). Inhibition of TDO results in increased TRP levels, and either TDO or KMO inhibition leads to a reduction in the 3-HK/KYNA ratio (highlighted in blue). The enzyme 3-hydroxyanthranilic acid dioxygenase is not present in flies, and thus QUIN is not synthesized.

Figure 2. TRP feeding ameliorates HTT93Q toxicity in fruit flies. (A) Rhabdomere quantification of HD flies treated with different concentrations of TRP during development. TRP concentrations higher than 0.4 mg/ml significantly ameliorate rhabdomere neurodegeneration. N = 6 – 13 per condition, *** P < 0.001. (B) The 3-HK/KYNA ratio is reduced in TRP fed HTT93Q flies. N = 5 – 6 per condition, *** P < 0.001. (C) TRP feeding rescues HTT93Q-dependent eclosion defects. Untreated HD flies: N = 938; TRP-treated HD flies: N = 728, *** P < 0.001. (D) TRP levels are significantly increased in $v^{-/-}$ HTT93Q flies compared to HTT93Q flies. N = 5 per condition, *** P < 0.001. (E) 3-HK/KYNA levels are reduced in $v^{-/-}$ HTT93Q compared to HTT93Q flies. N = 5 flies per condition, *** P < 0.001. (F) Treatment with the KAT inhibitor AOAA (100 µM in the food) reduces the level of KYNA in $v^{-/-}$ HTT93Q flies. N = 5 per condition. * P < 0.05. (G) AOAA treatment leads to a reduction in the 3-HK/KYNA ratio. N = 5 per condition, * P < 0.05. (H) KAT inhibition abrogates the neuroprotection conferred by the *v* mutation. N = 12 - 14 per condition, *** P < 0.001 and ns = not significant. (I) 3-HK feeding leads to increased levels of 3-HK in $v^{-/-}$ HTT93Q flies. N = 5 - 6 per treatment. *** P < 0.001 and ns = not significant. (J) 3-HK supplementation in the food of $v^{-/-}$ HTT93Q flies reduces neuroprotection compared to untreated HD flies. N = 8 – 12 per condition, *** P < 0.001 and ns = not significant. Data are the mean ± SEM (one-way ANOVA with Newman-Keuls *post hoc* test).

Figure 3. QUIN exacerbates neurodegeneration in HD flies and overexpression of human KAT (hKAT) is neuroprotective via increased KYNA levels. (A) QUIN levels in wild-type (WT) and HTT93Q-expressing flies. QUIN is detected in flies fed with 0.5 mg/ml of QUIN, but was not measurable in untreated flies. N= 3 - 5 flies per treatment, *** P < 0.001. (B) HTT93Q and *cn*$^{-/-}$HTT93Q flies fed QUIN exhibit increased rhabdomere degeneration compared to untreated flies. Neuroprotection conferred by the *cn* mutation is abolished by QUIN feeding. N = 11 - 12 per treatment, ** P < 0.01, *** P < 0.001. (C) Pan-neuronal overexpression of hKAT in a wild-type background causes an increase in KYNA production compared to controls at both post-eclosion ages tested. N = 3 - 5 per genotype, *** P < 0.001. (D) HTT93Q flies with pan-neuronal overexpression of hKAT show a significant reduction in the 3-HK/KYNA ratio. The transgene control used in this experiment was a transgenic *Drosophila* line expressing an empty pJFRC2 vector. N = 4 – 5 per condition, ** P< 0.01, *** P < 0.001. (E) Overexpression of hKAT is neuroprotective in HTT93Q flies at both post-eclosion ages tested. N = 9 – 13 flies per condition. ** P < 0.01 and *** P < 0.001. (F) Overexpression of hKAT ameliorates the eclosion phenotype observed in HTT93Q flies. Transgene control + Htt93Q flies: N = 1084; hKAT + Htt93Q flies: N = 1010. *** P < 0.001. ns = not significant. Data are the mean ± SEM (one-way ANOVA with Newman-Keuls *post hoc* test).

Figure 4. *v* and *cn* downregulation ameliorates PD- and AD-related impairments in *Drosophila*. Expression of aSyn (A) or $A\beta_{42ARC}$ (B) in motorneurons using the *c164*GAL4 driver reduces the distance crawled by third instar larvae. The silencing of *v* or *cn* significantly ameliorates these locomotor defects. N = 20 larvae per genotype. ** P < 0.01 and *** P < 0.001. Pan-neuronal expression of aSyn (C) or $A\beta_{42}$ (D) reduces average lifespan which is reversed by *v* and *cn* silencing. N = 100 per genotype. Median survival in days for aSyn experiments: UAS control = 86; RNAi Control + aSyn = 76; *v*RNAi + aSyn = 82; *cn*RNAi + aSyn = 81. Median survival in days for $A\beta_{42}$ experiments: UAS control = 84; RNAi Control + $A\beta_{42}$ = 54; *v*RNAi + $A\beta_{42}$ = 68; *cn*RNAi + $A\beta_{42}$ = 66. (E,F) Mean climbing pass rate at different post-eclosion ages for flies expressing aSyn or $A\beta_{42}$ pan-neuronally. Both aSyn (E) and $A\beta_{42}$ (F) reduce climbing performance, and the effects are reversed by downregulation of *v* and *cn*. N = 50 - 60 per genotype and condition. * P < 0.05 and *** P < 0.001. Pan-neuronal expression of $A\beta_{42Arc}$ reduces mean rhabdomeres per ommatidium (G); *v* and *cn* silencing protects rhabdomere degeneration at all post-eclosion ages tested. N = 7 - 11 per condition. ** P <

0.01 and *** P < 0.001. (H) The 3-HK/KYNA ratio is decreased in flies with RNAi down-regulation of *v* and *cn*. N = 5 per genotype. ** P < 0.01 and *** P < 0.001. Data are the mean ± SEM (one-way ANOVA with Newman-Keuls *post hoc* test).

Figure 5. Pharmacological inhibition of TDO is neuroprotective in HD, PD and AD flies. (A) Reduced neurodegeneration in HTT93Q flies treated with the TDO inhibitor 680C91 (100 µM) 7 days post-eclosion. N = 8 - 17 per condition. (B) aSyn and $A\beta_{42Arc}$ flies treated with 680C91 (100 µM) display improved climbing compared to controls. N = 50- 60 per genotype. DMSO = dimethyl sulfoxide. *** P < 0.001. ns = not significant. Data are the mean ± SEM (one-way ANOVA with Newman-Keuls *post hoc* test).

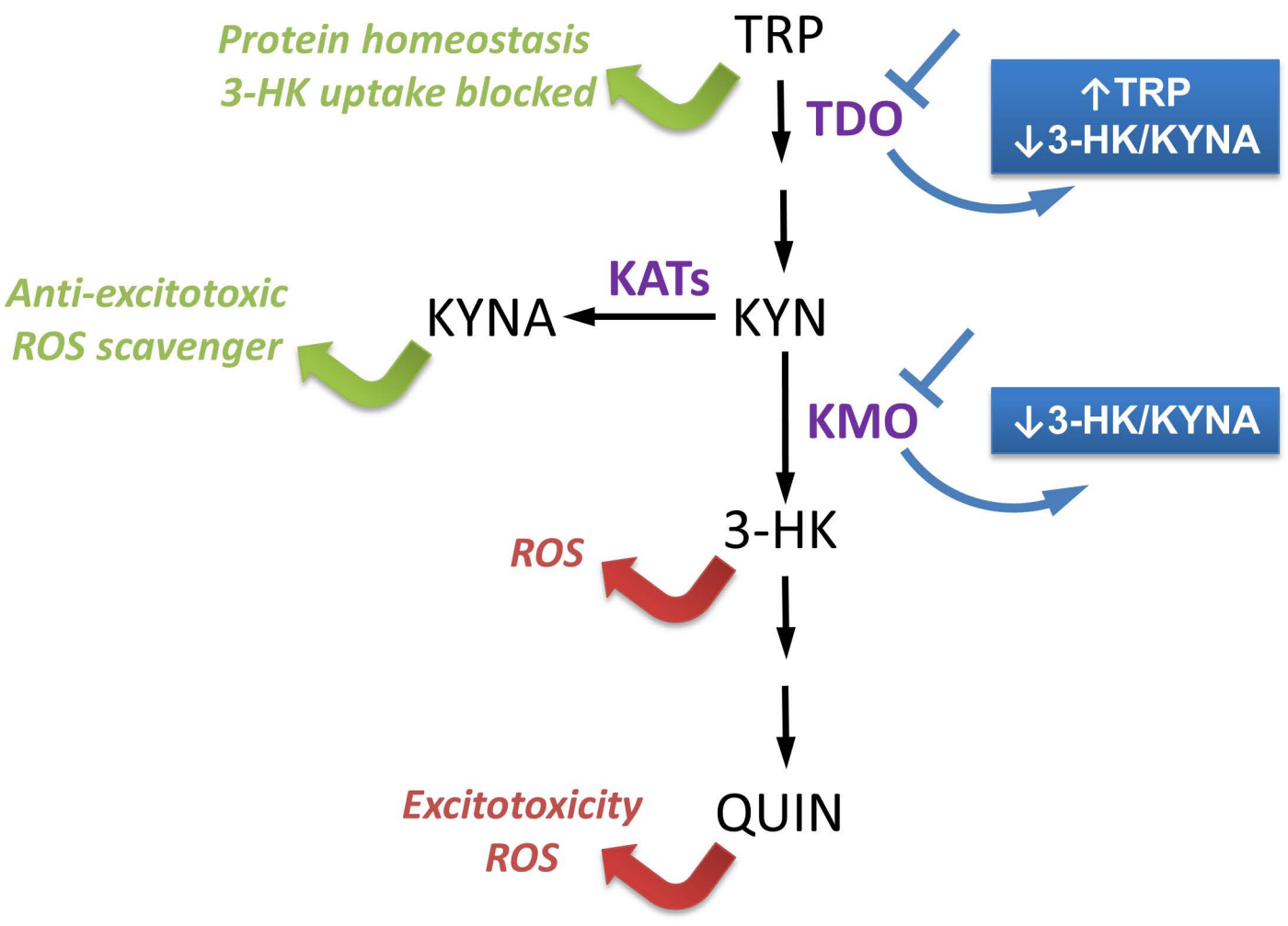
Protein homeostasis
3-HK uptake blocked
TRP
TDO
↑TRP
↓3-HK/KYNA
KATs
Anti-excitotoxic
ROS scavenger
KYNA
KYN
KMO
↓3-HK/KYNA
3-HK
ROS
QUIN
Excitotoxicity
ROS

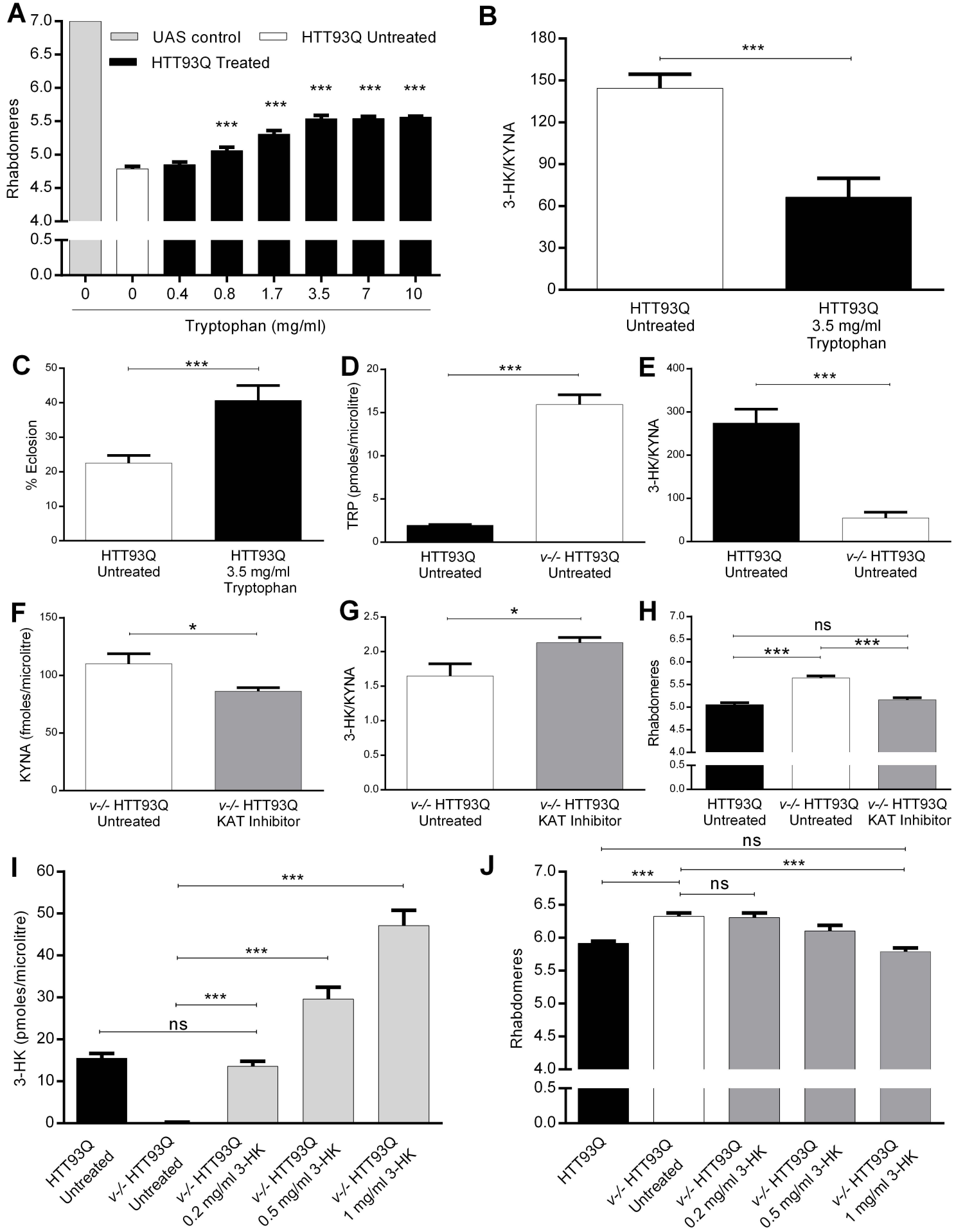
A
UAS control
HTT93Q Untreated
HTT93Q Treated
Rhabdomeres
Tryptophan (mg/ml)
0
0
0.4
0.8
1.7
3.5
7
10
B
3-HK/KYNA
HTT93Q Untreated
HTT93Q 3.5 mg/ml Tryptophan
C
% Eclosion
HTT93Q Untreated
HTT93Q 3.5 mg/ml Tryptophan
D
TRP (pmoles/microlitre)
HTT93Q Untreated
v-/- HTT93Q Untreated
E
3-HK/KYNA
HTT93Q Untreated
v-/- HTT93Q Untreated
F
KYNA (fmoles/microlitre)
v-/- HTT93Q Untreated
v-/- HTT93Q KAT Inhibitor
G
3-HK/KYNA
v-/- HTT93Q Untreated
v-/- HTT93Q KAT Inhibitor
H
Rhabdomeres
ns
HTT93Q Untreated
v-/- HTT93Q Untreated
v-/- HTT93Q KAT Inhibitor
I
3-HK (pmoles/microlitre)
ns
HTT93Q Untreated
v-/- HTT93Q Untreated
v-/- HTT93Q 0.2 mg/ml 3-HK
v-/- HTT93Q 0.5 mg/ml 3-HK
v-/- HTT93Q 1 mg/ml 3-HK
J
Rhabdomeres
ns
HTT93Q
v-/- HTT93Q Untreated
v-/- HTT93Q 0.2 mg/ml 3-HK
v-/- HTT93Q 0.5 mg/ml 3-HK
v-/- HTT93Q 1 mg/ml 3-HK

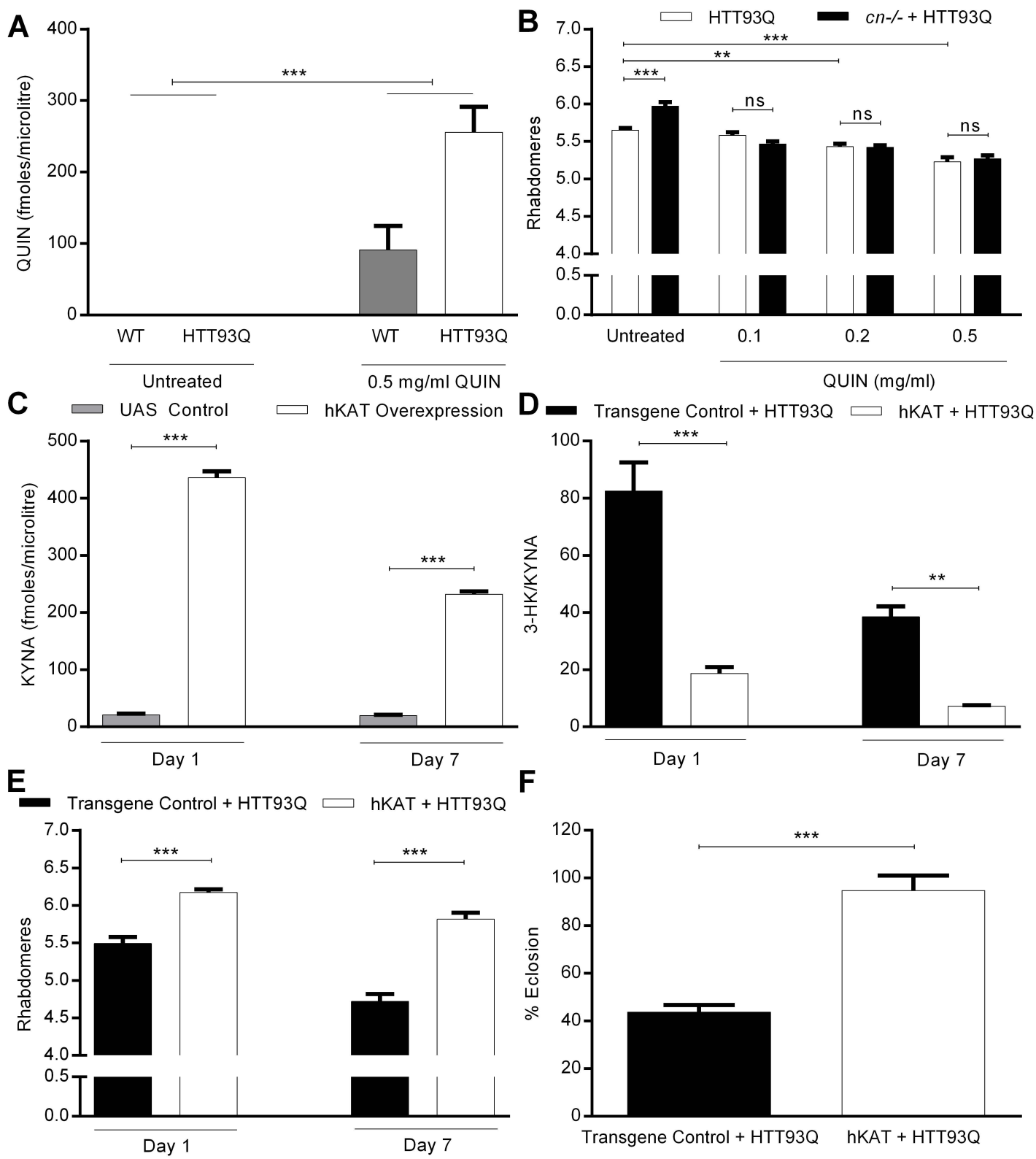
A
QUIN (fmoles/microlitre)
400
300
200
100
0
***
WT
HTT93Q
WT
HTT93Q
Untreated
0.5 mg/ml QUIN
B
HTT93Q
cn-/- + HTT93Q
Rhabdomeres
7.0
6.5
6.0
5.5
5.0
4.5
4.0
0.5
0.0
***
**
***
ns
ns
ns
Untreated
0.1
0.2
0.5
QUIN (mg/ml)
C
UAS Control
hKAT Overexpression
KYNA (fmoles/microlitre)
500
400
300
200
100
0
***
***
Day 1
Day 7
D
Transgene Control + HTT93Q
hKAT + HTT93Q
3-HK/KYNA
100
80
60
40
20
0
***
**
Day 1
Day 7
E
Transgene Control + HTT93Q
hKAT + HTT93Q
Rhabdomeres
7.0
6.5
6.0
5.5
5.0
4.5
4.0
0.5
0.0
***
***
Day 1
Day 7
F
% Eclosion
120
100
80
60
40
20
0
***
Transgene Control + HTT93Q
hKAT + HTT93Q

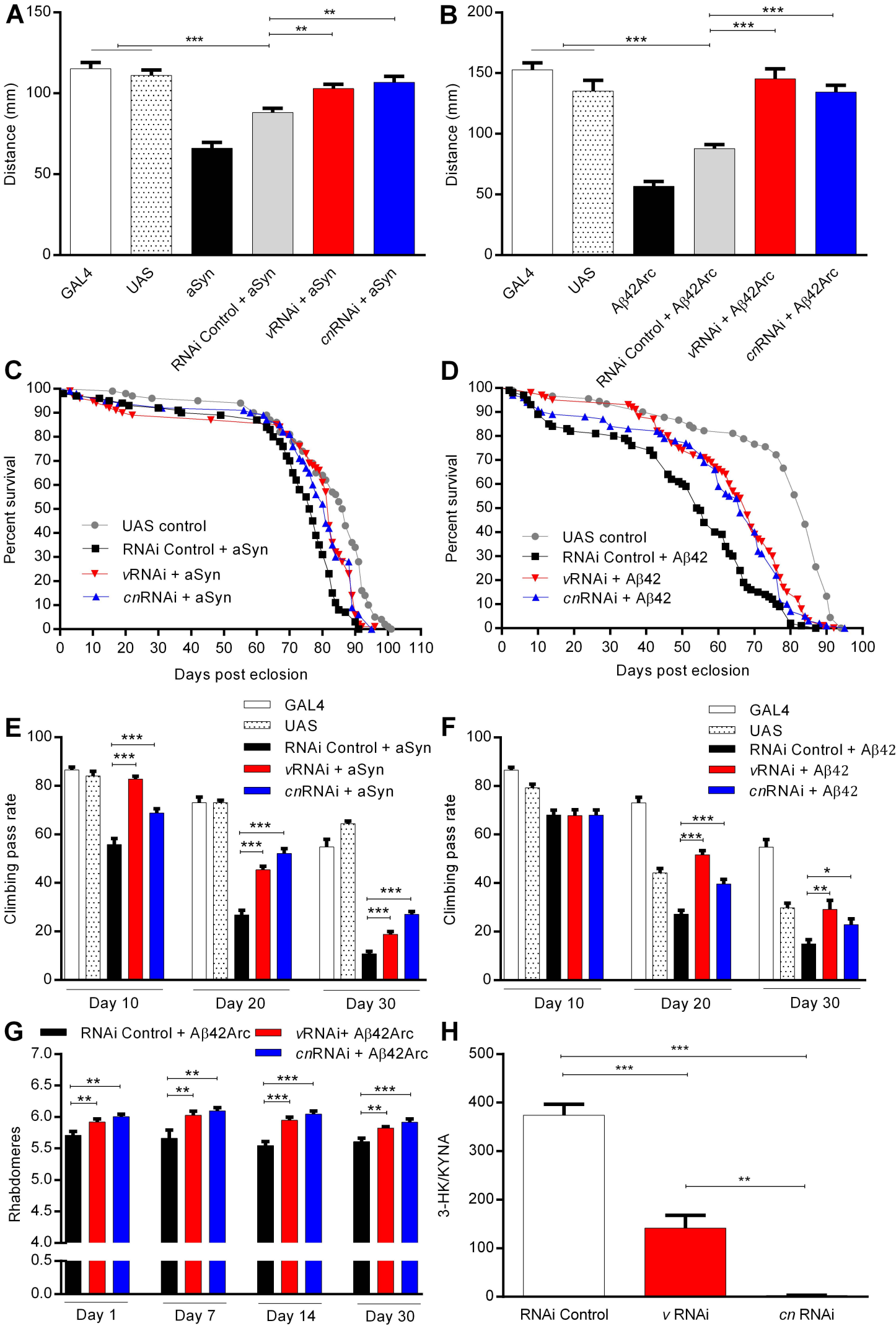
A
Distance (mm)
GAL4
UAS
aSyn
RNAi Control + aSyn
vRNAi + aSyn
cnRNAi + aSyn
B
Distance (mm)
GAL4
UAS
Aβ42Arc
RNAi Control + Aβ42Arc
vRNAi + Aβ42Arc
cnRNAi + Aβ42Arc
C
Percent survival
UAS control
RNAi Control + aSyn
vRNAi + aSyn
cnRNAi + aSyn
Days post eclosion
D
Percent survival
UAS control
RNAi Control + Aβ42
vRNAi + Aβ42
cnRNAi + Aβ42
Days post eclosion
E
GAL4
UAS
RNAi Control + aSyn
vRNAi + aSyn
cnRNAi + aSyn
Climbing pass rate
Day 10
Day 20
Day 30
F
GAL4
UAS
RNAi Control + Aβ42
vRNAi + Aβ42
cnRNAi + Aβ42
Climbing pass rate
Day 10
Day 20
Day 30
G
RNAi Control + Aβ42Arc
vRNAi+ Aβ42Arc
cnRNAi + Aβ42Arc
Rhabdomeres
Day 1
Day 7
Day 14
Day 30
H
3-HK/KYNA
RNAi Control
v RNAi
cn RNAi

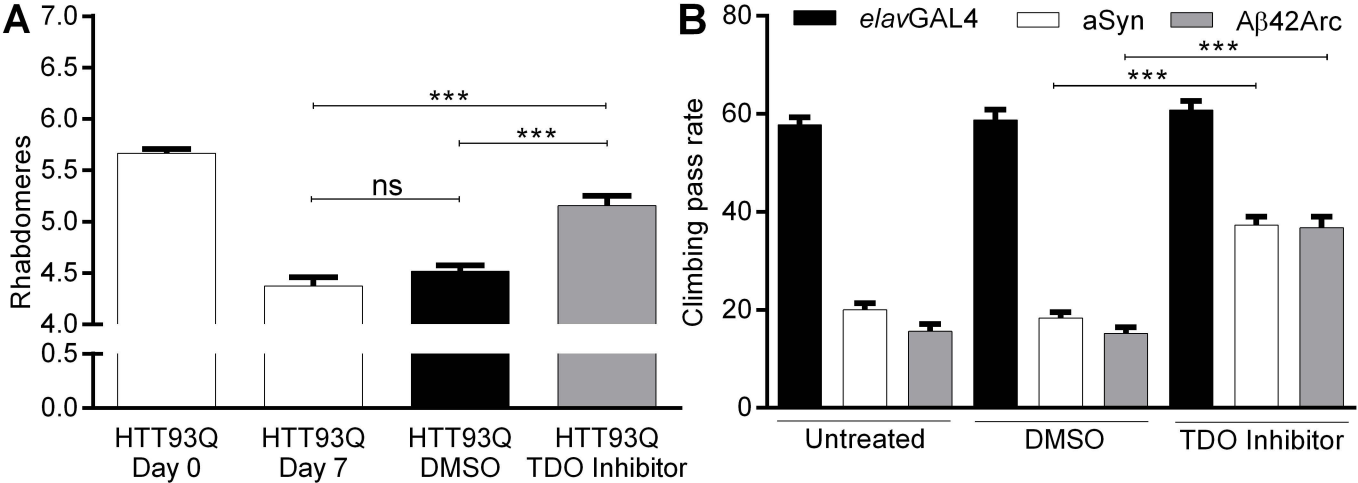
A
Rhabdomeres
7.0
6.5
6.0
5.5
5.0
4.5
4.0
0.5
0.0
***
***
ns
HTT93Q Day 0
HTT93Q Day 7
HTT93Q DMSO
HTT93Q TDO Inhibitor
B
elavGAL4
aSyn
Aβ42Arc
Climbing pass rate
80
60
40
20
0
***
***
Untreated
DMSO
TDO Inhibitor

SUPPLEMENTAL INFORMATION

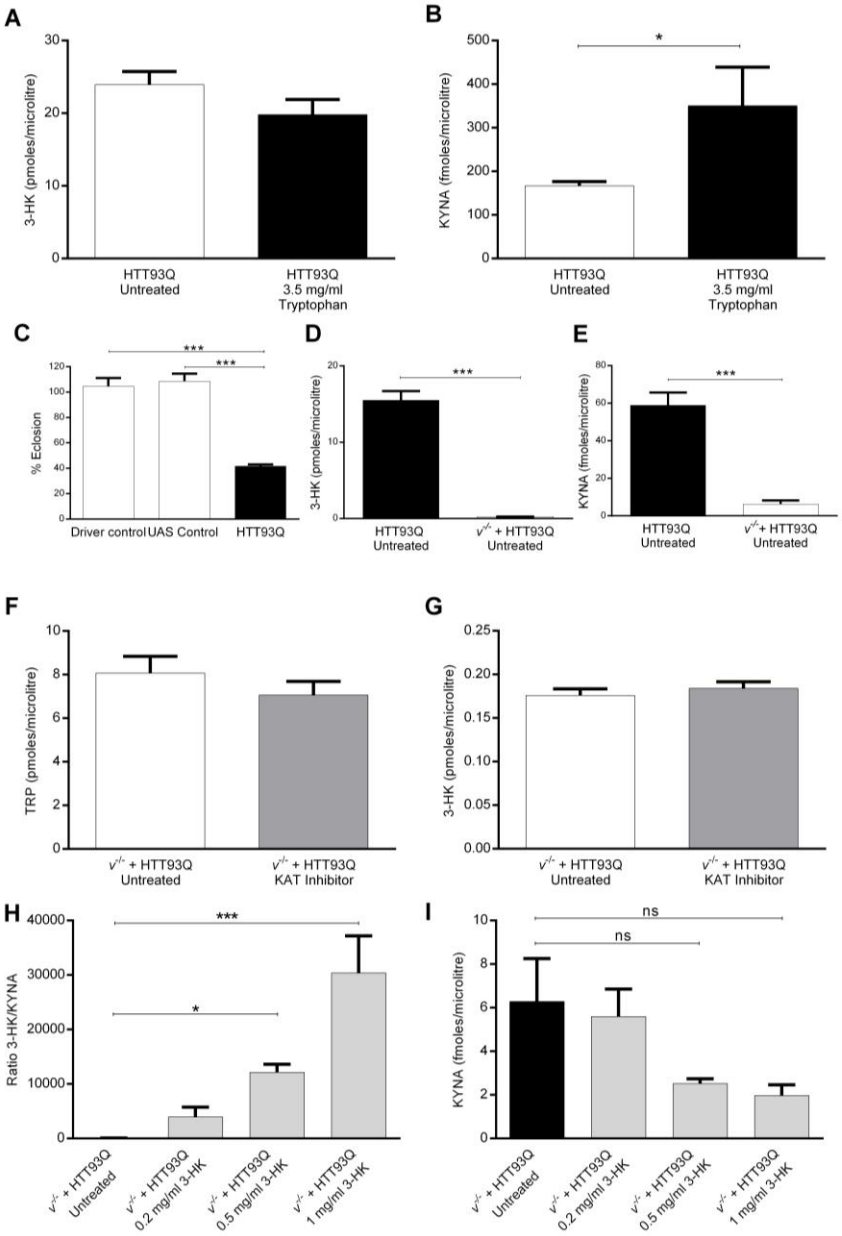

Figure S1. Levels of KP metabolites in HTT93Q and *v*$^{-/-}$ HTT93Q flies treated with TRP or 3-HK. (A) No significant difference in 3-HK levels is observed between untreated and TRP-treated Htt93Q flies. *n* = 5 - 6 per condition. (B) TRP fed Htt93Q flies display a higher level of KYNA compared to untreated controls. *n* = 5 - 6 per condition. * P < 0.05. (C) The frequency of eclosion in HD flies is significantly reduced compared to controls. Driver control flies: *n* = 1437; UAS control flies: *n* = 1066; HD flies; *n* = 1216. *** P < 0.001. *v*$^{-/-}$ HTT93Q flies show a decreased level of 3-HK (D) and KYNA (E). *n* = 5 per condition. *** P < 0.001. TRP (F) and 3-HK (G) levels are not affected by the administration of the KAT inhibitor AOAA (100 µM in the food). *n* = 5 per condition. (H) The 3-HK/KYNA ratio is increased in *v*$^{-/-}$ HTT93Q flies fed with 3-HK. *n* = 5 – 6 per condition, * P < 0.05 and *** P < 0.001. (I) No significant difference in KYNA levels is observed in *v*$^{-/-}$ HTT93Q flies treated with increasing concentrations of 3-HK. *n* = 5 - 6 per condition. Data are the mean ± SEM (one-way ANOVA with Newman-Keuls *post hoc* test).

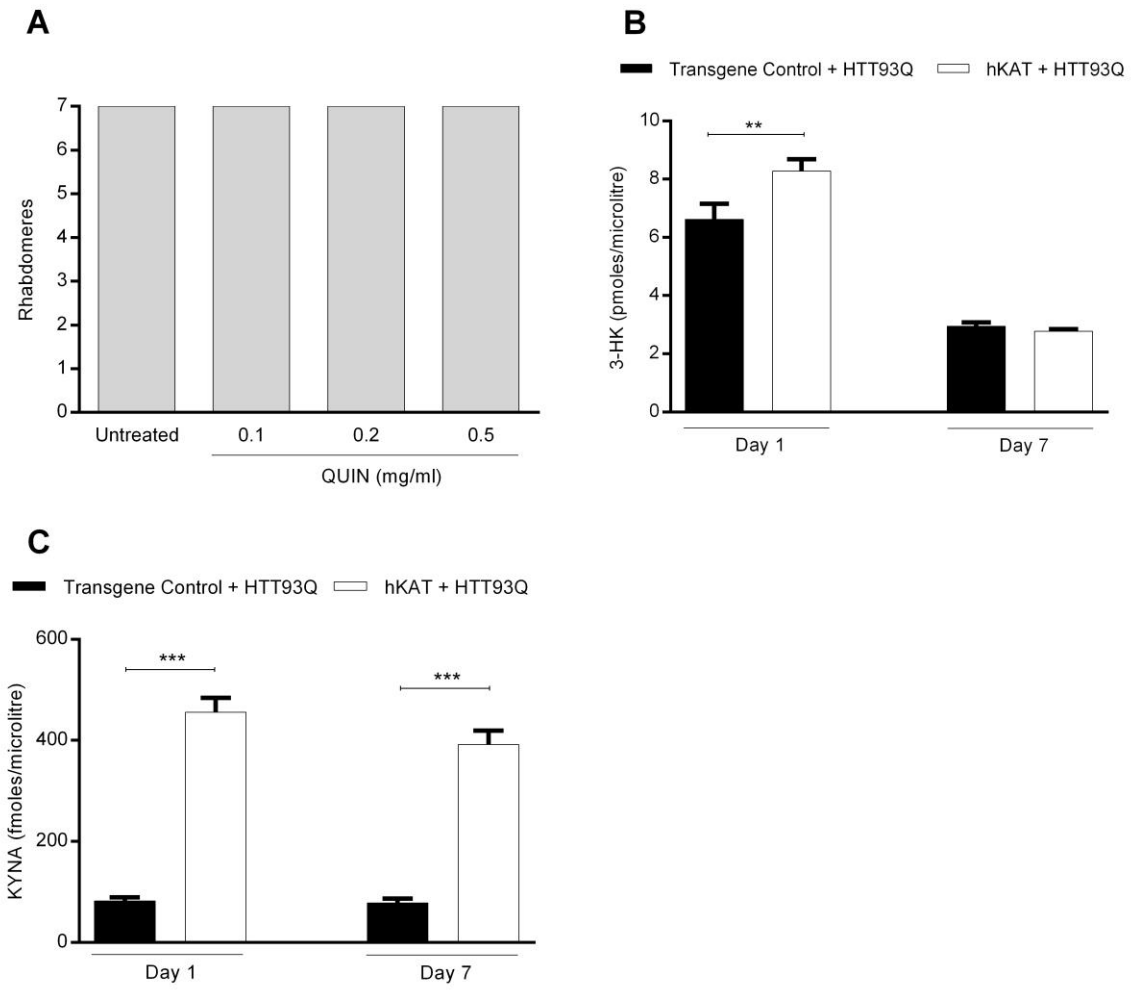

Figure S2. (A) QUIN feeding does not lead to neurodegeneration in wild-type flies. Wild-type flies fed with increasing concentrations of QUIN do not exhibit rhabdomere degeneration compared to untreated flies. *n* = 6 – 7 per condition. **(B, C) Levels of 3-HK and KYNA in flies overexpressing hKAT.** Days 1 and 7. *n* = 4 - 5 per condition. ** P < 0.01 and *** P < 0.001. Data are the mean ± SEM (one-way ANOVA with Newman-Keuls *post hoc* test).

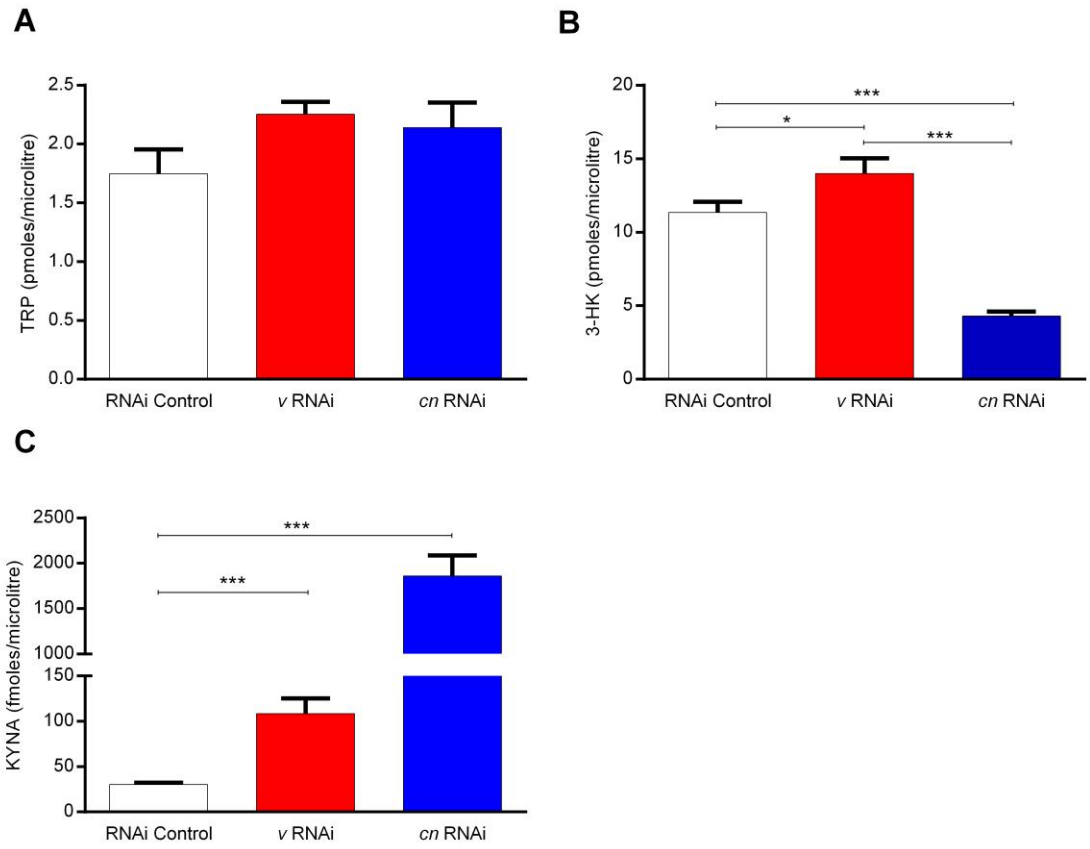

Figure S3. *v* and *cn* silencing alters levels of KP metabolites. (A) TRP levels are unaltered in flies down-regulating *v* and *cn* compared to the RNAi control. *n* = 5 per genotype. (B) The level of 3-HK is significantly increased in *v* RNAi and decreased in *cn* RNAi flies. *n* = 5 per genotype. * $P < 0.05$ and *** $P < 0.001$. (C) KYNA levels are increased in both *v* and *cn* RNAi lines compared to the control. *n* = 5 per genotype. *** $P < 0.001$. Data are the mean ± SEM (one-way ANOVA with Newman-Keuls *post hoc* test).

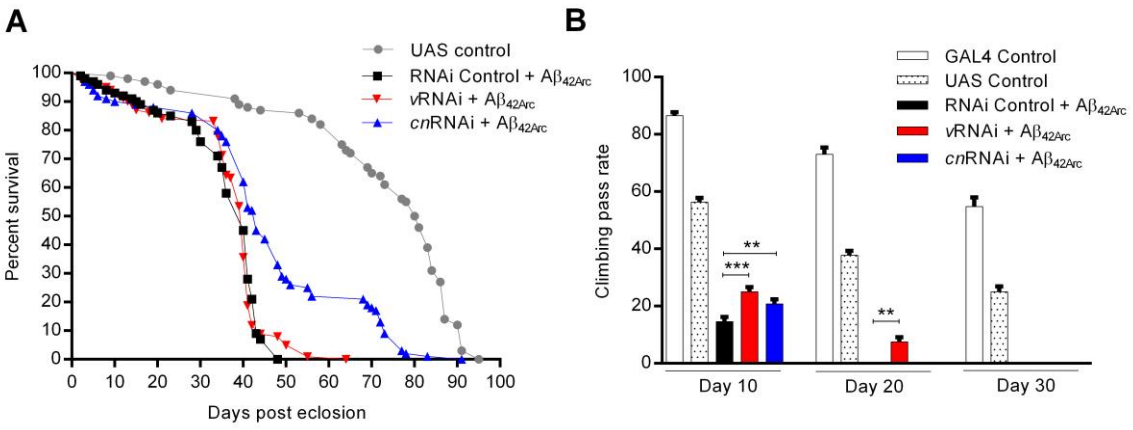

Figure S4. *v* and *cn* silencing in aβ$_{42Arc}$-expressing flies improves diseases-related phenotypes. (A) Survival curve of flies expressing Aβ42Arc pan-neuronally and down-regulating *v* and *cn*. The silencing of *cn* ameliorates decreased lifespan observed in flies. *n* = 100 per genotype. (B) Mean climbing pass rate at different post-eclosion ages of flies expressing Aβ$_{42Arc}$ pan-neuronally. Aβ$_{42}$ reduces climbing, which is significantly rescued by the downregulation of *v* or *cn* at day 10 post-eclosion. *n* = 50 - 60 per genotype and condition. ** $P < 0.01$ and *** $P < 0.001$. Data are the mean ± SEM (one-way ANOVA with Newman-Keuls *post hoc* test).

Materials and Methods

Pseudopupil analysis

Visible rhabdomeres were scored from 50-150 ommatidia per fly at day 0 or 7 post-eclosion using the scoring method published previously (1). Aged fly heads were fixed to slides using fingernail polish, and rhabdomeres were examined at 500 X magnification using a Nikon Optiphot-2 microscope (1).

Eclosion analysis

Eclosion in the fly lines was assessed as described previously (2). Briefly, males carrying the sex-linked *elav*GAL4 driver were crossed to virgin females homozygous for the *UAS-HTT93Q* transgene generating experimental females and control males in the F1 generation. Flies were allowed to lay eggs on vials with or without treatment, and the number of adult females and males emerging from the pupal case in each vial was counted every day for 9 days. Eclosion percent was determined by the following calculation: (number of female flies/number of male flies)*100.

Feeding experiments

Tryptophan (Sigma-Aldrich, St. Louis, MO, USA) was dissolved in water and subsequently added to the standard food at several concentrations (0.4, 0.8, 1.7, 3.5, 7 and 10 mg/ml). 3-HK (Sigma-Aldrich) and QUIN (Sigma-Aldrich) were dissolved in water and then mixed with standard maize food at the concentrations of 1 mg/ml (3-HK) or 0.1, 0.2 and 0.5 mg/ml (QUIN). Crosses were set up on the supplemented media, and rhabdomeres were scored at day 0 (newly emerged adult flies). The non-specific KAT inhibitor aminooxyacetic acid (AOAA) - also referred to as O-(Carboxymethyl)hydroxylamine hemihydrochloride – from Sigma-Aldrich was dissolved in water whereas the TDO inhibitor 680C91 (Tocris Bioscience, Bristol, UK) was dissolved in dimethyl sulfoxide (DMSO; 0.001% final). Compounds were added to maize media at 100 µM (final concentration). Flies were introduced to the media upon eclosion, supplemented media were changed every day, and rhabdomeres were scored after 7 days of treatment.

Measurement of KP metabolites

Ten fly heads were homogenized by sonication in 100 µl of ultrapure water, and the homogenate was further diluted (1:10, v/v) in ultrapure water. One hundred µl of the preparation were then thoroughly mixed with 25 µl of 6% perchloric acid, and the precipitated proteins were removed by centrifugation (16,000 x g, 15 min). For the determination of KYNA, the resulting supernatant was further diluted 1:10 (v/v) with ultrapure water, and 20 µl were subjected to HPLC analysis. KYNA was isocratically eluted from a 3 µm C_{18} reverse-phase column (HR-80; 80 mm x 4.6 mm, ESA, Chelmsford, MA, USA), using a mobile phase containing 0.25 M zinc acetate, 50 mM sodium acetate and 3% acetonitrile (pH adjusted to 6.2 with glacial acetic acid) at a flow rate of 1 ml/min and was then quantitated fluorimetrically (excitation: 344 nm, emission: 398 nm; Perkin Elmer Series 200, Waltham, MA, USA). The retention time of KYNA was ~7 min. For the measurement of 3-HK, the deproteinized supernatant was either used directly or diluted (1:10 or 1:20, v/v) with ultrapure water, and 20 µl of the solution were applied to a 3 µm C_{18} reverse-phase column (HR-80; 80 mm x 4.6 mm, ESA), using a mobile phase containing 1.5% acetonitrile, 0.9% triethylamine, 0.59% phosphoric acid, 0.27 mM EDTA and 8.9 mM sodium heptane sulfonic acid. 3-HK was isocratically eluted at a flow rate of 0.5 ml/min and detected electrochemically using a HTEC 500 detector (Eicom Corp., San Diego, CA; oxidation potential: +0.5 V). The retention time of 3-HK was ~11 min.

For the measurement of TRP, the deproteinized supernatant was further diluted 1:100 (v/v) with ultrapure water, and 20 µL were subjected to HPLC analysis. TRP was isocratically eluted from a 3 µm C_{18} reverse phase HPLC column (150 mm × 4 mm; Dr. Maisch GmbH, Ammerbuch, Germany), using a mobile phase containing 50 mM sodium acetate and 5% acetonitrile (pH adjusted to 6.2 with glacial acetic acid) at a flow rate of 0.5 ml/min. Zinc acetate, 0.5 M (not pH adjusted), was delivered post column by a peristaltic pump (Dionex AXP, Thermo Fisher, Waltham, MA, USA) at a flow rate of 0.1 ml/min. In the eluate, TRP was detected fluorimetrically (excitation: 365 nm, emission: 385 nm; S200a fluorescence detector; Perkin Elmer). The retention time of TRP was ~7 min.

QUIN levels were quantified by GC/MS/MS. To this end, 10 fly heads were homogenized by sonication in 100 µl of ultrapure water, and the homogenate was further diluted (1:10, v/v)

in 0.1 % ascorbic acid. 50 µl of a solution containing internal standard ([$^2H_3$]QUIN) were added to 50 µl of the respective sample, and proteins were precipitated with 50 µL of acetone. After centrifugation (13,700 x g, 5 min), 50 µl of methanol:chloroform (20:50) were added to the supernatant, and the samples were centrifuged (13,700 x g, 10 min). The upper layer was added to a glass tube and evaporated to dryness (90 min). The samples were then derivatized with 120 µl of 2,2,3,3,3-pentafluoro-1-propanol and 130 µl of pentafluoropropionic anhydride at 75°C for 30 min, dried down again and reconstituted in 50 µl of ethyl acetate. One µl was injected into the gas chromatograph. GC/MS analysis was carried out with a 7890A GC coupled to a 7000B MS/MS (Agilent Technologies, Santa Clara, CA, USA), using electron capture negative chemical ionization (3).

Behavioral assays

For larval crawling experiments, crosses were set up on standard maize fruit fly food mixed with 0.05% Bromophenol Blue (FisherBiotech, Loughborough, UK) as described previously (4). Briefly, deeply blue colored third instar wandering larvae were washed in distilled water, and the distance covered by larvae in 2 min was manually tracked on a transparent paper placed on the top of the petri dish lid. The tracks were scanned, and the distance calculated using ImageJ (5).

Negative geotaxis assays were performed as previously described (4). Briefly, flies of the desired genotype were placed in a cylinder with a diameter of 2.3 cm and a total length of 18.4 cm. Before the experiment, flies were left to acclimatize for 1 min. For each trial, the tubes were tapped gently in order to gather the flies at the bottom. The flies were then allowed to fly or scale the sides of the tube for 10 sec, and the number of flies which passed an 8 cm height threshold was recorded. The same cohort of flies was re-tested 10 times. In between climbing trials, the flies were allowed to rest for 1 min. This process was repeated on days 10, 20 and 30 post-eclosion.

Longevity analysis

Virgin females of the desired genotype were collected and kept in groups of 10 in separate vials. Vials were inspected and changed every 2-3 days, and the number of flies remaining alive was scored.

Statistical analyses

Statistical analyses were performed using Prism 6 (GraphPad Software). Analyses were carried out using ANOVA with the Newman–Keuls *a posteriori* test. For longevity, survival curves were generated and data were analysed using the Kaplan–Meier method and log-rank statistics.

References

1. Campesan S*, et al.* (2011) The kynurenine pathway modulates neurodegeneration in a Drosophila model of Huntington's disease. *Curr Biol* 21(11):961-966.
2. Varadarajan S*, et al.* (2015) The transrepression arm of glucocorticoid receptor signaling is protective in mutant huntingtin-mediated neurodegeneration. *Cell Death Differ* 22(8):1388-1396.
3. Notarangelo FM, Wu HQ, Macherone A, Graham DR, & Schwarcz R (2012) Gas chromatography/tandem mass spectrometry detection of extracellular kynurenine and related metabolites in normal and lesioned rat brain. *Anal Biochem* 421(2):573-581.
4. Breda C*, et al.* (2015) Rab11 modulates alpha-synuclein-mediated defects in synaptic transmission and behaviour. *Hum Mol Genet* 24(4):1077-1091.
5. Schneider CA, Rasband WS, & Eliceiri KW (2012) NIH Image to ImageJ: 25 years of image analysis. *Nat Methods* 9(7):671-675.